Acta Cryst. (1995). D**51**, 760–766

X-ray Structure Determination of a Dimeric Hemoglobin from *Caudina arenicola*

BY DAVID T. MITCHELL,* STEPHEN R. ERNST AND MARVIN L. HACKERT†

Department of Chemistry and Biochemistry, University of Texas at Austin, Austin, TX 78712, USA

(*Received* 29 *August* 1994; *accepted* 31 *January* 1995)

Abstract

The X-ray structure of a dimeric, cyanomet-liganded hemoglobin D-chain (Hb-D) from *Caudina arenicola* has been determined by the molecular-replacement method. The search model was a concatenated model of three hemoglobin structures superimposed on the backbone of monomeric, hemichrome hemoglobin C-chain (Hb-C) from the same organism. Hb-D crystallizes in space group $P4_12_12$ with cell constants $a = b = 77.0$ and $c = 61.5$ Å with one subunit in the asymmetric unit. The dimer twofold axis corresponds to a crystallographic twofold along one of the body diagonals of the unit cell. Rotation and translation searches as well as model refinement were carried out in *X-PLOR* with the final model having an R value of 0.19 using the data from 5.0 to 2.9 Å resolution ($R = 0.26$ for 10.0 to 2.9 Å resolution). The homodimeric structure of *Caudina* Hb-D features close heme-heme contacts with an Fe—Fe distance of 19.0 Å. The subunit–subunit interface involves both the E and F helices from each subunit with the E helices oriented antiparallel at 50° with respect to one another, similar to the quaternary structure observed for the homodimeric hemoglobin from *Scapharca inaequivalvis*.

Introduction

The oxyhemoglobins found in nucleated erythrocytes in the coelomic fluid of the sea cucumber, *Caudina arenicola*, are cooperative hetero- and homodimers composed of four different globin chains referred to as Hb-A, Hb-B, Hb-C and Hb-D. We have previously reported the structure of a monomeric, hemichrome hemoglobin C-chain (Hb-C) determined at 2.5 Å resolution by the multiple isomorphous replacement (MIR) method (Mitchell, Ernst, Wu & Hackert, 1995). The most interesting aspects of the *Caudina* hemoglobins are the 'ligand-linked' dissociation and the cooperativity of oxygen binding by the hemoglobin chains. Deoxy forms of the *Caudina* hemoglobins exist as tetramers or higher oligomers (Whitfill, 1973). The oxy, carbonmonoxy and cyanomet-liganded hemoglobin forms are dimeric. Heterodimers from *Caudina* hemoglobins exhibit enhanced cooperativity of oxygen binding ($n = 1.45$; $P_{50} = 8.0$ mm Hg), especially when one D subunit is present. Homodimers are themselves slightly cooperative, unlike human α and β hemoglobins (Bonaventura, Bonaventura, Kitto, Brunori & Antonini, 1976). The methemoglobins are monomeric at all observed protein concentrations (Bonaventura & Kitto, 1993).

We report here the X-ray structure of the cooperative, cyanomet-liganded homodimer of Hb-D from *C. arenicola*. The X-ray structure retains the classic 'myoglobin fold' but the D helix is absent in the Hb-D structure, similar to human α hemoglobin. The tertiary and quaternary structures of Hb-D are similar to the homodimeric carbonmonoxy-liganded *Scapharca inaequivalvis* hemoglobin (Royer, Hendrickson & Chiancone, 1989; Royer, 1994). The molecular-replacement solution for the Hb-D structure was aided by the use of a concatenated search model of four hemoglobin subunits.

Materials and methods

Hemoglobin D (Hb-D) was purified from nucleated red blood cells found in the coelomic cavity of *C. arenicola* (Mauri, Omnaas, Davidson, Whitfill & Kitto, 1991) and crystallized from PEG with Hb-D at a protein concentration of 7 mg ml^{-1} in phosphate buffer with KCN at pH 7.0 as previously described (Carson, Bowers, Kitto & Hackert, 1979). Native and derivative data sets were collected on a Syntex four-circle goniostat equipped with a Picker X-ray generator and a *KRISEL CONTROL* automation package. Intensity data were obtained using a modified ω-scan mode. The scan rate was constant at 1.5° min^{-1} with 1.5 min per reflection and a background to peak count time ratio of 0.4. Three standard reflections were measured after every 100 reflections to monitor crystal and instrument stability. Intensities were corrected for crystal decay and absorption corrections were applied using an empirical φ-scan approach. Intensities were further corrected for Lorentz and polarization effects.

The rotation-function and translation searches outlined in Table 1 were carried out using *X-PLOR*, Version 2.1 (Brünger, Kuriyan & Karplus, 1987) employing a 2σ cutoff on the data within 15.00 to 4.0 Å resolution

* Current Address: Department of Biochemistry 4-225 Millard Hall, University of Minnesota, 435 Delaware Street SE, Minneapolis, MN 55455-0326, USA.

† Author to whom all correspondence should be addressed.

Table 1. *Summary of the molecular-replacement solution of Hb-D*

Patterson vectors between 4 and PV Å were used to calculate the RF correlation coefficient. The ψ, φ, κ angles, as defined in *X-PLOR*, of the concatenated Hb model (con-Hb) and translation solution of Hb-D in the $P4_12_12$ space group gave a model that packed in the unit cell, refined and produced a reasonable NED electron-density map.

Model	Resolution range (Å)	PV (Å)	Rotation ψ	φ	κ	Translation x	y	z	R factor	R Min	NED map
Hb-C	10.0–4.5	12.0	62.22	28.94	129.19		Packing constraints				
Hb-C efh	10.0–6.0	10.0	53.59	9.02	129.78	$P4_1$ 0.447	0.104	0.754	0.56	0.34	Poor
Hb-'D'	10.0–5.0	17.0	81.10	40.88	103.20	$P4_1$ 0.211	0.026	0.213	055	0.33	Poor
Hb-C	15.0–4.0	20.0	71.84	52.41	168.92	$P4_1$ 0.395	0.312	0.918	0.56	0.34	Poor
						$P4_3$ 0.145	0.948	0.492	0.57	0.34	
Hb-'D'	15.0–4.0	20.0	65.34	40.06	176.91	$P4_1$ 0.224	0.247	0.262	0.56	0.34	Poor
						$P4_3$ 0.289	0.623	0.836	0.55	0.35	Poor
con-Hb	15.0–4.0	25.0	68.95	43.47	183.05	$P4_1$ 0.250	0.584	0.525	0.49	—	—
						$P4_3$ 0.250	0.597	0.770	0.53	—	—
Hb-'D'	15.0–4.0	25.0	68.95	43.47	183.05	$P4_1$ 0.250	0.597	0.541	0.54	0.26	Good
						$P4_3$ 0.092	0.169	0.492	0.58		

ranges, and radii of integration ranging from 10.0 to 30.0 Å. The search model was a 'concatenated Hb' model with monomers of *Urechis caupo* hemoglobin (Kolatkar *et al.*, 1991), human β hemoglobin (Fermi, Perutz, Shaanan & Fourme, 1984), and *S. inaequivalvis* hemoglobin (Royer *et al.*, 1989) superimposed on the Hb-C chain monomer (Fig. 1). Model refinement was carried out initially using the same version of *X-PLOR* running on a Cray Y-MP8/864 and later with *X-PLOR* Version 3.1 (Brünger, 1992) running on a Silicon Graphics Crimson workstation. Initial refinement was carried out from 10.0 to 3.0 Å resolution (2748 reflections) and included energy minimization and simulated annealing from a starting temperature of 3000 K. Later refinement used the shell of data from 5.0 to 2.9 Å resolution (2009 reflections) and also included individual temperature-factor refinement. However, the X-ray weighting parameter calculated in *X-PLOR* and used in refinement was usually cut in half to favor the contribution of the geometric parameters during refinement.

Manual rebuilding of the model was carried out using *FRODO* (Jones, 1979) running on an Evans and Sutherland PS 390 or *O* (Jones, Zou, Cowan & Kjeldgaard, 1991) on a Silicon Graphics Crimson workstation. To minimize model bias, NED (non-existent density) electron-density maps generated by the program *NEDFFT* (Main, 1979; Kolatkar *et al.*, 1991) were used for manual rebuilding of the model. OMIT maps calculated by *X-PLOR* were also used as an aid during rebuilding. Solvent molecules were placed in the X-ray model using $(F_o - F_c)$ difference electron-density peaks greater than 3σ above background.

Results

The octahedral crystals of dimeric, cyanomet liganded Hb-D belong to space group $P4_12_12$ with $a = b = 77.0$, $c = 61.5$ Å and one half of the dimer in the asymmetric unit, thus the molecular twofold of the dimer lies along the body diagonal of the unit cell. Earlier attempts to solve the structure of Hb-D by means of MIR techniques were unsuccessful due to a lack of isomorphism of the derivatives or shinkage of the unit-cell c axis when crystals were soaked in heavy-metal solutions (Carson, 1980). Data sets were recollected on 'shrunk' native and derivative crystals, but the resulting low-resolution difference Fourier maps were still uninterpretable (Carson, 1980). Attempts to solve the translation problem by determining the Fe-atom positions from an anomalous difference Patterson were also unsuccessful (Carson, 1980).

With the recent solution of monomeric, hemichrome Hb-C from the same organism (Mitchell *et al.*, 1995) and the strong sequence homology (McDonald, Davidson & Kitto, 1992; Mauri *et al.*, 1991) between Hb-C and Hb-D (102/157 amino-acid identities), a molecular-replacement solution for Hb-D was attempted. Somewhat surprisingly, molecular-replacement 'solutions' based on a search model of *Caudina* Hb-C, or a 'Hb-D' which had the Hb-D amino-acid sequence modeled on the Hb-C backbone, or *Scapharca* hemoglobin, yielded models with R values as low as 0.22 following *X-PLOR* refinement, but these models were rejected on the basis of either packing constraints or poor quality of the resulting NED electron-density maps. Table 1 summarizes some of the rotation and translation searches

carried out using *X-PLOR*. Following the approach used by Leahy *et al.* (Leahy, Axel & Hendrickson, 1992) to solve the structure of human CD8 by molecular replacment, a concatenated hemoglobin model was constructed. The resulting rotation angles (the last two rows of Table 1) were consistent over several resolution ranges using different radii of integration (Brünger *et al.*, 1987). Translation-function searches were carried out both in the $P4_12_12$ and $P4_32_12$ space groups, with both the *R* factor and quality of electron-density maps calculated after energy minimization clearly favoring the 4_1 space group.

Refinement of the model began at the rotation angles and translation positions indicated in the final row of Table 1 with the Hb-D amino-acid sequence on the Hb-C backbone. The final model was arrived at by repeated rounds of refinement and model building. Difference Fourier maps calculated at 3σ above background were relatively flat throughout the entire molecule, except for five solvent molecules that are present in the current model. The *R* value of the current model using the 5.0 to 2.9 Å resolution shell of data is 0.19 and the r.m.s. deviations from ideal geometry (*X-PLOR*) are as follows: bond lengths 0.016 Å, bond angles 3.6°, dihedral angles 24.3° and improper angles 1.7°. Fig. 2 is a ribbon drawing of the Hb-D dimer with the molecular twofold nearly perpendicular to the plane of the page showing the overall 'myoglobin fold' of the Hb-D subunit and a dimer interface consisting of the *E* and *F* helices from each subunit.

Fig. 3 is a Ramachandran plot (Ramachandran & Sasisekharan, 1968) showing the φ, ψ torsion angles for the final Hb-D model. The outliers are residues in the N and C terminii and *CD* loop region, presumably caused by the poorly defined nature of the electron density in these regions. None of the outliers are among the residues in the seven helical regions of Hb-D. The extended N- and C-terminal tails are longer that those found in many invertebrate hemoglobins. Affinity chromatography has shown that met Hb-D is approximately 2% glycosylated (McDonald, 1991). The electron density and amino-acid sequence suggest that the N- (Ser5, Gln7, Ser8) and C- (Lys155, Ser158) terminal regions and the *EF* turn (Asp89, Thr90, Glu91) region could be the glycosylated region of this molecule, but the current resolution of the data preclude a more complete analysis.

Fig. 4. is a stretch of the *B* helix with its corresponding electron density (upper 10%) which is indicative of the helical density for this model at 2.9 Å resolution. Fig. 5 is a plot of the temperature factors (Å^2) for both main- and side-chain atoms as a function of residue number. The average temperature factors for specific groups are as follows: all protein atoms 19.4 Å^2, main-chain atoms 21.9 Å^2, side-chain atoms 16.9 Å^2, heme-group atoms 23.3 Å^2, and cyanide ligand 13.7 Å^2. The temperature factors for the main-chain atoms in the N-terminal region are large because of crystal contacts between neighboring acetyl groups. The helical regions with the lowest temperature factors are helices *E–G* which are involved in the Hb-D dimer interface.

The seven helices of the Hb-D structure form regular α-helices with the standard $n+4$ hydrogen bonding. Like the Hb-C globin chain, Hb-D is acetylated at the N terminus (Kitto, Erwin, West & Omnaas, 1976). The recent cDNA sequence of Hb-D (Thomas, 1994) corrected two errors in the protein amino-acid sequence reported previously (Mauri *et al.*, 1991). Residues 2–4 should be in the order Ala-Thr-Gln instead of Gln-Ala-Thr and position 48 is a Thr instead of Trp. The long N-terminal tail begins near the end of the *H* helix and does not exhibit any regular secondary structure. The *A* helix begins with Thr13, which is a highly conserved residue at that position, contains the highly conserved Trp at position 24, and ends at Met28. The *B* helix begins at Thr32 and runs through to Asn45. The *B*10 position which forms part of the distal heme pocket is Phe39, flanked by Val35 and Phe43. The *C* helix starts with a β-turn at Asp46 and runs to Lys52. The *CD* loop region begins with the highly conserved Phe53 (*CD*1) in the heme pocket but otherwise lacks any recognizable secondary-structural elements. There is no *D* helix, even though the hemichrome Hb-C structure does possess a *D* helix and Hb-C and Hb-D chains are quite similar in this region (Mitchell *et al.*, 1995). The *D* helix is also absent from the dimeric *Scapharca* hemoglobin (Royer *et al.*, 1989). The long *E* helix begins at Arg68, includes the distal histidine (*E*7) at 73, has a slight kink in its helix near the molecular twofold at Arg76, contains Val77 at position *E*11, and continues to Asp86. The Hb-D *EF* turn region contains two extra residues compared to human β hemoglobin, but one fewer residues than *Scapharca* hemoglobin. The *F* helix hegins at Val92, includes the proximal histidine (*F*8) at 104, ends at Asn107, and is somewhat distorted due to the presence of Pro94. The Nδ1 atom of His104 makes a hydrogen bond (2.8 Å) with the carbonyl O atom of Leu100 (2.8 Å apart) as also observed in many other hemoglobin X-ray structures. The side chain of Tyr84 (*E*18) is folded 'out' rather than 'in' as found in the Hb-C structure and may effect the *F* helix between resides 98 and 100. The fit of the *F/G* turn region was rather difficult because of the nature of its electron density, but the beginning of the *G* helix at Gly110 is very clear. The *G* helix runs until Glu128 with the *H* helix beginning at Thr134 and ending at Val148. The long C-terminal extensions lack any secondary-structural elements except for the possibility of a β-turn between Val148 and Leu152.

The distal side of the heme group of Hb-D features many large hydrophobic residues, as also observed for Hb-C (Fig. 6). Thes residues include Phe39 at *B*10 and Ile42 from the *B* helix, the highly conserved Phe53 at position 1 in the *CD* region, His73 at *E*7 and Val77 at *E*11 in the *E* helix and Phe117 from the *G* helix. Distance

and angle measurements on the heme region were performed using *X-RAY*76 (Stewart, 1976), *FRODO* (Jones, 1979), and *O* (Jones *et al.*, 1991). The mean plane of the four pyrrole N atoms is tipped 4° out of the mean plane of the porphyrin ring. The Fe atom is 0.5 Å out of these mean planes, similar to the out-of-plane distance for deoxyhemoglobin. The distance from His104 Nε1 to the Fe atom is 2.0 Å and the distance from the Fe atom to the C atom of the cyanide ligand is 1.8 Å. By comparison, the values for cyanomet liganded *Urechis caupo* hemoglobin are 2.17 Å (constrained during refinement) and 1.77 Å, respectively (Kolatkar, Hackert & Riggs, 1994).

Cyanide ligand binding to porphyrins in small molecules and in proteins has been studied for many years (Deatherage, Loe, Anderson & Moffat, 1976). In the cases of globin molecules the results for cyanomyoglobin (Bretscher, 1968), cyanomet lamprey hemoglobin (Hendrickson & Love, 1971), and horse cyanomethemoglobin, the ligand binds with a 'bent geometry', that is non-colinear with the normal to the mean heme plane. The Fe—C—N bond angle for Hb-D is 156° and was not constrained during refinement. As a test, this angle was set to 180° before refinement, but returned to 160° during refinement. This indicates a bent-ligand binding geometry for the cyanomet-liganded Hb-D chain. Errors in the atom coordinates are in the neighborhood of 0.2 Å for a protein model at this resolution.

The dimeric structure of Hb-D brings the two heme groups in close proximity and has subunit–subunit contacts involving the *E* and *F* helices of each subunit with the *E* and *E'* helices oriented antiparallel at 50° to one another (Fig. 7). The quarternary structure is similar to that observed for the homodimer from *S. inaequivalvis* (clam) (Royer *et al.*, 1989). The Hb-D dimer interface consists of hydrophobic interactions involving residues in the *E* and *F* helices. Val77 and Val77′, Ala79 and Ala79′, along with Ile75 and Leu96′ lie nearest the molcular twofold. Other hydrophobic interactions in this region involve Ala72, Leu80, Val92 and Leu 93. Electrostatic interactions are seen primarily between Gln69 OE1 and Glu95′ OE2; Glu91 OE1 and Arg68′ NH1; Arg76 and Heme159 O2A′; and Arg 102 and Heme159 O2D′. Difference Fourier maps with magnitude $(F_o - F_c)$ led to the placement of five solvent molecules in the X-ray model. As can be seen in Fig. 2 two of the solvent molecules lie in the dimer interface region with one molecule positioned between the side chain of Arg76 and the heme A propionate arm from the same subunit. The second solvent molecule in the interface region lies near Lys106 at the end of the *F* helix. The solvent molecule in the *A/B* turn region lies in

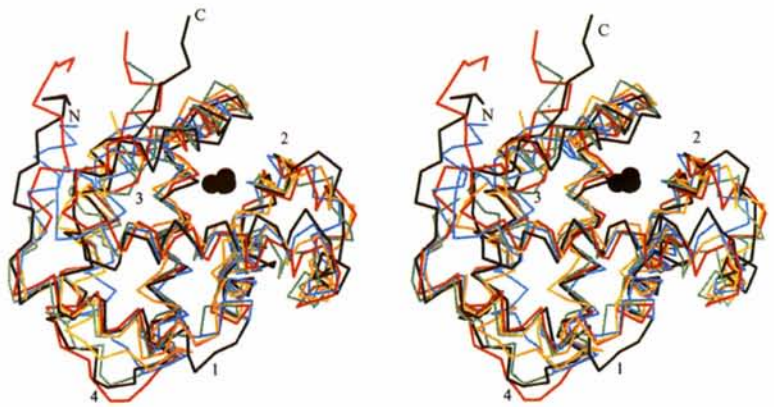

Fig. 1. Cα representation of the concatenated Hb model (*MOLSCRIPT*; Kraulis, 1991). *Urechis* Hb (yellow), human β Hb (green), *Scapharca* Hb (cyan), and Hb-C (black). The major areas of difference are the N and C terminii, *A/B* turn (1), *CD* loop region (2), *E/F* turn (3), and *G/H* turn (4). The Hb-D model is also superimposed and shown in red.

Fig. 2. Stereoview of the Hb-D dimer with the molecular twofold nearly perpendicular to plane of the page (*MOLSCRIPT*; Kraulis, 1991). The dimer interface is made up of close heme–heme contacts and the *E* and *F* helices of each subunit with the *E* helices running antiparallel with respect to one another (solvent molecules shown as blue spheres).

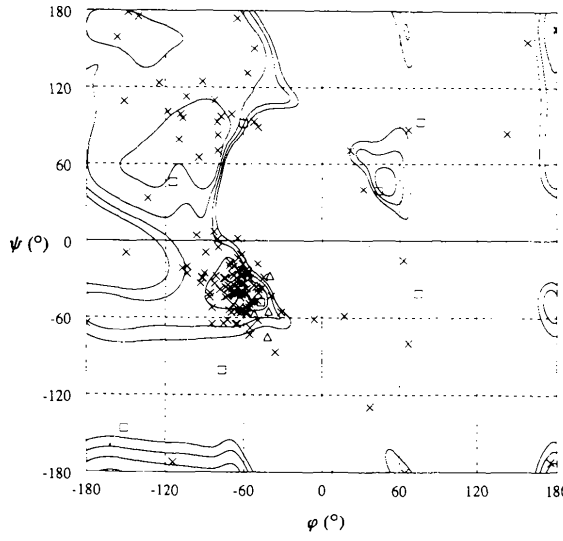

Fig. 3. Ramachandran plot of Hb-D (triangles are Pro, squares are Gly). The outlying residues are in the *CD* region and N- and C-terminal extensions.

a similar position to a solvent molecule in the Hb-C X-ray structure from the same organism (Mitchell *et al.*, 1994). The fourth solvent molecule lies near Gln69 at the beginning of the *E* helix, while the last solvent molecule is near the *CD* region.

Discussion

The three-dimensional structure of a cooperative, cyanomet dimeric hemoglobin, Hb-D from *C. arenicola*, has been determined by molecular-replacement methods at a resolution of 2.9 Å. Overall, the secondary and tertiary structure of liganded Hb-D and hemichrome Hb-C from *C. arenicola* are similar. As expected, the *E* helix moves farther from the heme group compared with its position in the hemichrome Hb-C structure, but, unexpectedly, the *D* helix present in Hb-C is absent from Hb-D. Other differences in the loop and terminal regions may play a role in the 'ligand-linked' dissociation observed for hemoglobins from this organism

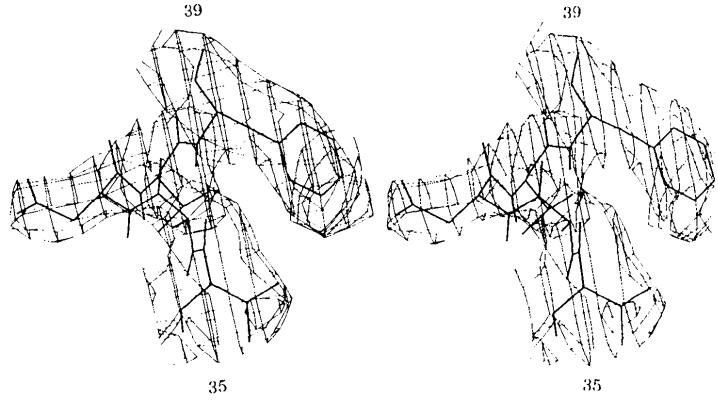

Fig. 4. NED electron density for a turn of the *B* helix contoured to show the top 10% of the density and the fit of the Hb-D model.

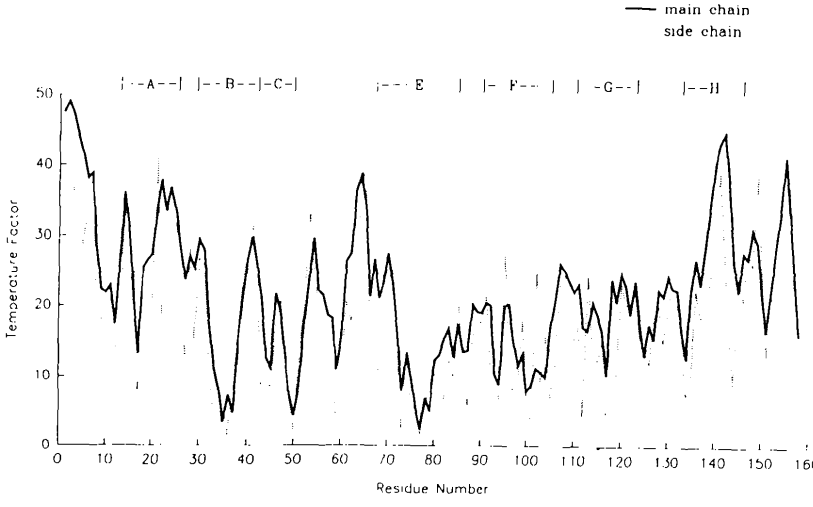

Fig. 5. Plot of temperature factors (Å^2) *versus* residue number for Hb-D. The seven helical regions are indicated above the plot.

(Bonaventura *et al.*, 1976). With regards to ligand binding, the cyanide ligand binds to the Fe atom of the heme group at an angle from the normal to the mean plane of the pyrrole N atoms and overall mean plane of the heme group. In addition the Fe atom out-of-plane distance is quite large for a liganded hemoglobin model although a higher resolution X-ray model would be needed to analyze this feature in detail. The dimer interface is made from the two heme groups and *E* and *F* helices of each subunit with the *E* helices running antiparallel with respect to one another at an angle of 50°.

The quaternary structure observed for Hb-D is similar to that reported for the cooperative, carbonmonoxy liganded, dimeric hemoglobin from *S. inaequivalvis* (Royer *et al.*, 1989; Royer, 1994). The overall similarity of these two dimeric hemoglobins is very interesting from an evolutionary point of view since the two species belong to very different invertebrate phyla. The similarities include the close heme–heme contacts and the subunit–subunit interface involving the *E* and *F* helices from each subunit. The Fe–Fe distance is 19.0 Å in Hb-D and 17.6 Å in *Scapharca* hemoglobin. Interestingly, the *D* helix is absent in both Hb-D and *Scapharca* hemoglobins even though the hemichrome model of Hb-C does possess a *D* helix. Recently, the X-ray structure of myoglobin from yellowfin tuna (*Thunnus albacares*) has been reported (Birnbaum, Evans, Przybylska & Rose, 1994) and it too lacks a *D* helix which has been attributed to the loss of a salt bridge and hydrogen bond. Work with human hemoglobin removing the *D* helix from the β subunit or inserting it into the α subunit has shown no effect with regard to ligand-binding affinity (Komiyama, Shih, Looker, Tame & Nagai, 1991).

Some unique features of the *Caudina* Hb-D X-ray model can be found as well. The long N- and C-terminal extensions are rather unusual even for an invertebrate hemoglobin. The path of the main chain for the *Caudina* Hb-D through the *EF* turn and beginning of the *F* helix is much different from *Scapharca* hemoglobin, possibly due to the presence of the pre-*A* helix in *Scapharca* hemoglobin. Even though the dimer interfaces for both Hb-D and *Scapharca* involve the *E* and *F* helices and the same types of interactions, the residues that interact along the dimer interface appear to be quite different. In the case of Hb-D, a pair of arginine residues (76 and 102) from the *E* and *F* helices interact with the propionate arms of the heme group from the neighboring subunit. In the case of *Scapharca* hemoglobin, it is believed that a Phe from the *F* helix is directly involved in oxygen affinity and that two *F*-helix residues (Lys and Asn) are responsible for heme–heme communication.

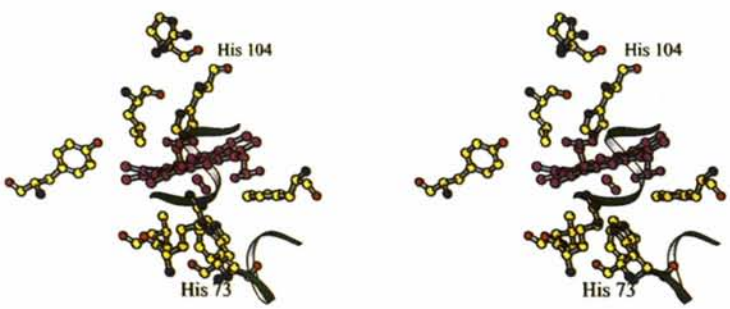

Fig. 6. Close-up view of the Hb-D heme region showing the ligand coordination and the conserved residues indicated in their positions of the Hb-D heme pocket.

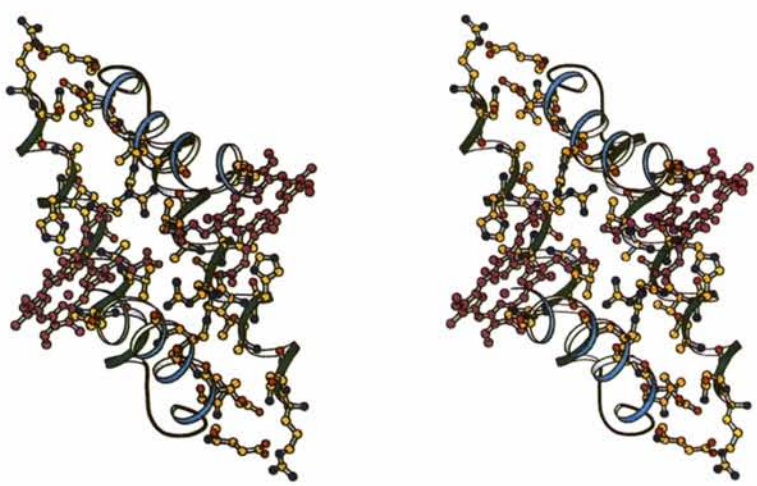

Fig. 7. Ball-and-stick model of the Hb-D dimer interface (*MOLSCRIPT*; Kraulis, 1991) with the *E* helices in green, *F* helices in light blue, and heme groups in purple. Note the large number of hydrophobic residues as well as electrostatic interactions along the interface.

Attempts to improve the resolution of this crystal form have thus far been unsuccessful. However, an orthorhombic crystal form of Hb-D has been obtained and diffraction data collected to 2.6 Å resolution. Self-on-self and self-on-model rotation searches have been carried out using the current model. A set of peaks has been found using the Tanaka rotation-function program (Tanaka, 1977) for monomeric and dimeric Hb-D self-on-model rotation searches that are consistent and obey the crystallographic symmetry constraints of the orthorhombic system. Translation-function searches are currently being carried out based on these results. Work is also underway to crystallize the deoxy form of this hemoglobin. It is hoped that the new higher resolution model of Hb-D and the future availability of the deoxy structure will aid in obtaining a more detailed picture of the quarternary structure and deeper understanding of the functional properties of these invertebrate hemoglobins.

The authors would like to thank Dr Prasanna Kolatkar for ideas on molecular-replacement solutions and Dr G. Barrie Kitto for suggesting the project and ideas on developing the manuscript. MLH gratefully acknowledges partial support for this project from grants from NIH (GM 30105) and the Robert A. Welch Foundation.

References

BIRNBAUM, G. I., EVANS, S. V., PRZYBYLSKA, M. & ROSE, D. R. (1994). *Acta Cryst.* D**50**, 283–289.

BONAVENTURA, C., BONAVENTURA, J., KITTO, B., BRUNORI, M. & ANTONINI, E. (1976). *Biochim. Biphys. Acta*, **428**, 779–786.

BONAVENTURA, J. & KITTO, G. B. (1973). In *Comparative Physiology*, edited by L. BOLIS, K. SVHMIDT-NIELSON & S. H. P. MADDRELL. Amsterdam: North-Holland.

BRETSCHER, P. A. (1968). PhD thesis, Univ. of Cambridge, England.

BRÜNGER, A. T. (1992). *X-PLOR*. Yale Univ. Press, New Haven, Conneticut, USA.

BRÜNGER, A., KURIYAN, J. & KARPLUS, M. (1987). *Science*, **235**, 458–460.

CARSON, W. M. (1980). PhD Dissertation, Univ. of Texas, Austin, Texas, USA.

CARSON, W. M., BOWERS, T. T., KITTO, G. B. & HACKERT, M. L. (1979). *J. Biol. Chem.* **254**, 7400–7402.

DEATHERAGE, J. F., LOE, S. R., ANDERSON, C. M. & MOFFAT, K. (1976). *J. Mol. Biol.* **104**, 687–706.

FERMI, G., PERUTZ, M. F. SHAANAN, B. & FOURME, R. (1984). *J. Mol. Biol.* **175**, 159–174.

HENDRICKSON, W. A. & LOVE, W. E. (1971). *Nature (London)*, **232**, 197–203.

JONES T. A. (1979). *J. Appl. Cryst.* **11**, 268–272.

JONES, T. A., ZOU, J. Y., COWAN, S. W. & KJELGAARD, M. (1991). *Acta Cryst.* A**47**, 110–119.

KITTO, G. B., ERWIN, D., WEST, R. & OMNAAS, J. (1976). *Comp. Biochem. Physiol. B*, **55**, 105–107.

KOLATKAR, P., ERNST, S. R., HACKERT, M. L., OGATA, C. M., HENDRICKSON, W. A., MERRITT, R. & PHIZACKERLEY, R. P. (1991). *Acta Cryst.* B**48**, 191–199.

KOLATKAR, P. R., HACKERT, M. L. & RIGGS, A. F. (1994). *J. Mol. Biol.* **237**, 87–97.

KOMIYAMA, N. H., SHIH, D. T.-B., LOOKER, D., TAME, J. & NAGAI, K. (1991). *Nature* (London), **352**, 349–351.

KRAULIS, P. J. (1991). *J. Appl. Cryst.* **24**, 946–950.

LEAHY, D. J., AXEL, R. & HENDRICKSON, W. A. (1992). *Cell*, **68**, 1145–1162.

MCDONALD, G. D. (1991). PhD dissertation, Univ. of Texas, Austin, Texas, USA.

MCDONALD, G. D., DAVIDSON, L. & KITTO, G. B. (1992). *J. Protein Chem.* **11**, 29–37.

MAIN, P. (1979). *Acta Cryst.* A**35**, 779–785.

MAURI, F., OMNAAS, J., DAVIDSON, L. WHITFILL, C. & KITTO, G. B. (1991). *Biochem Biophys. Acta*, **1078**, 63–67.

MITCHELL, D. T., ERNST, S. R., WU, W.-X. & HACKERT, M. L. (1995). *Acta Cryst.* D**51**, 647–653.

RAMACHANDRAN, G. N. & SASISEKHARAN, V. (1968). *Adv. Protein Chem.* **246**, 3356–3366.

ROYER, W. E. (1994). *J. Mol. Biol.* **235**, 657–681.

ROYER, W. E., HENDRICKSON, W. A. & CHIANCONE, E. (1989) *J. Biol. Chem.* **264**, 21052–21061.

STEWART, J. M. (1976). Editor. *XRAY*76, Univ. of Maryland, College Park, Maryland, USA.

TANAKA, N. (1977). *Acta Cryst.* A**23**, 191–193.

THOMAS, P. W. (1994). PhD dissertation, Univ. of Texas, Austin, Texas, USA.

WHITFILL, C. (1973). PhD dissertation, Univ. of Texas, Austin, Texas, USA.